

1 **Obtaining the three-dimensional structure of tree orchards from**  
2 **remote 2D terrestrial LIDAR scanning.**

3

4 **Joan R. Rosell<sup>1,\*</sup>, Jordi Llorens<sup>4</sup>, Ricardo Sanz<sup>1</sup>, Jaume Arnó<sup>1</sup>, Manel Ribes-Dasi<sup>1</sup>,**  
5 **Joan Masip<sup>1</sup>, Alexandre Escolà<sup>1</sup>, Ferran Camp<sup>3</sup>, Francesc Solanelles<sup>3</sup>, Felip Gràcia<sup>3</sup>,**  
6 **Emilio Gil<sup>4</sup>, Luis Val<sup>5</sup>, Santiago Planas<sup>1</sup>, Jordi Palacín<sup>2</sup>.**

7

8 <sup>1</sup>Department of Agro-forestry Engineering, University of Lleida, Av. Rovira Roure 191,  
9 25198 Lleida, Spain

10 <sup>2</sup>Department of Informatics and Industrial Engineering, University of Lleida, Av. Jaume II  
11 69, 25197 Lleida, Spain

12 <sup>3</sup>Centre de Mecanització Agrària. Agriculture, Food and Rural Action Department.  
13 Generalitat de Catalunya. Av. Rovira Roure 191, 25198 Lleida, Spain

14 <sup>4</sup>Department of Agri Food Engineering and Biotechnology, Politechnical University of  
15 Catalunya, Campus del Baix Llobregat, edifici D4, Av. del Canal Olímpic, s/n. 08860  
16 Castelldefels, Spain

17 <sup>5</sup>Department of Mechanization and Agricultural Technology, Politechnical University of  
18 Valencia, Camino de Vera, s/n. 46020, Valencia, Spain

19

---

\* Corresponding author: Joan Ramon Rosell Polo. Department of Agro-forestry  
Engineering, Universitat de Lleida, Avinguda Rovira Roure 191, 25198 Lleida, Spain  
Phone: +34-973-702861, Fax: +34-973-238264, Email: jr.rosell@eagrof.udl.cat

20 **ABSTRACT**

21

22 In recent years, LIDAR (Light Detection and Ranging) sensors have been widely used to  
23 measure environmental parameters such as the structural characteristics of trees, crops and  
24 forests. Knowledge of the structural characteristics of plants has a high scientific value due  
25 to their influence in many biophysical processes including, photosynthesis, growth, CO<sub>2</sub>-  
26 sequestration and evapotranspiration, playing a key role in the exchange of matter and  
27 energy between plants and the atmosphere, and affecting terrestrial, above-ground, carbon  
28 storage. In this work, we report the use of a 2D LIDAR scanner in agriculture to obtain  
29 three-dimensional (3D) structural characteristics of plants. LIDAR allows fast, non-  
30 destructive measurement of the 3D structure of vegetation (geometry, size, height, cross-  
31 section, etc). LIDAR provides a 3D cloud of points, which is easily visualized with  
32 Computer Aided Design software. Three-dimensional, high density data are uniquely  
33 valuable for the qualitative and quantitative study of the geometric parameters of plants.  
34 Results are demonstrated in fruit and citrus orchards and vineyards, leading to the  
35 conclusion that the LIDAR system is able to measure the geometric characteristics of plants  
36 with sufficient precision for most agriculture applications. The developed system made it  
37 possible to obtain 3D digitalized images of crops, from which a large amount of plant  
38 information -such as height, width, volume, leaf area index and leaf area density- could be  
39 obtained. There was a great degree of concordance between the physical dimensions, shape  
40 and global appearance of the 3D digital plant structure and the real plants, revealing the  
41 coherence of the 3D tree model obtained from the developed system with respect to the real  
42 structure. For some selected trees, the correlation coefficient obtained between manually  
43 measured volumes and those obtained from the 3D LIDAR models was as high as 0.976.

44

45

46 Key words: Terrestrial LIDAR, Laser measurements, 3D Plant structure, Tree volume,  
47 Geometrical characteristics of plants, Plant modelling.

48

## 49 **1. Introduction**

50 Considering the structural aspects of a canopy is important at different scales: individual  
51 tree, crop, forest and ecosystem. Foliar spatial arrangement determines the possibilities for  
52 resource capture and atmospheric exchange (Phattaralerphong and Sinoquet, 2004). Plant  
53 structure influences many biophysical processes including, photosynthesis, growth, CO<sub>2</sub>-  
54 sequestration and evapotranspiration (Li et al., 2002; Pereira et al., 2006). At the forest  
55 level, structure plays a key role in the exchange of matter and energy between plants and  
56 the atmosphere, and affects terrestrial, above-ground, carbon storage (Van der Zande et al.,  
57 2006). Aspects of structure can indicate stand developmental stage and its potential for  
58 growth, and may also help to predict attributes that are important in stand management,  
59 such as stem density, basal area, and above-ground biomass (Parker et al., 2004).  
60 Vegetation structure and diversity are also essential factors that influence habitat selection  
61 for animal species in forest ecosystems (Bradbury, 2005).

62

63 In recent decades, several innovative remote sensing methods have been developed to  
64 characterize the 3D structure of individual trees or tree canopies. The use of ultrasonic  
65 sensors (Giles et al., 1988; Zaman and Salyani, 2004; Zaman and Schumann, 2005;  
66 Solanelles et al., 2006), photography (Phattaralerphong and Sinoquet, 2004, Leblanc et  
67 al.,2005), stereo images (Rovira-Más et al., 2005; Andersen et al., 2005, Kise and Zhang,

68 2005), light sensors (Giuliani et al., 2000), high-resolution radar images (Bongers, 2001)  
69 and high-resolution X-ray computed tomography (Stuppy et al., 2003) offers innovative  
70 solutions to the task of structural assessment, although most of these methods pose practical  
71 problems under field conditions (Van der Zande et al., 2006).

72

73 LIDAR (**L**ight **D**etection and **R**anging) laser technology potentially provides a relatively  
74 novel tool for generating a unique and comprehensive quantitative description of plant  
75 structure. LIDAR is a non-destructive remote sensing technique for measuring distances.  
76 The distance between the sensor and the target (e.g. leaf, branch) can be measured by two  
77 alternative methods: i) measuring the time that a laser pulse takes to travel between the  
78 sensor and the target (*time-of-flight LIDAR*) or ii) measuring the phase difference between  
79 the incident and reflected laser beams (*phase-shift measurement LIDAR*). A LIDAR system  
80 is able to create 3D structural datasets with high point densities from which structural  
81 variables can be extracted in a computer environment. Many published studies have been  
82 based on LIDAR measurements of forest canopy structure, ranging from terrestrial systems  
83 beneath the canopy (Fleck et al., 2004; Fröhlich et al., 2004, Aschoff et al., 2004; Pfeifer et  
84 al., 2004), to airborne systems (Naesset, 1997a,b; Blair et al., 1999; Lee et al., 2004;  
85 Solberg et al., 2004; Tanaka et al., 2004; Yu et al., 2005; Houldcroft et al., 2005; Coops et  
86 al., 2007; Naesset, 2008, 2009).

87

88 Forestry was one of the first disciplines to use 3D information extracted from remote  
89 sensing data (aerial photographs) to produce three-dimensional models of trees and  
90 canopies. Since 1933, stereo-photogrammetry has been known as a suitable technology not  
91 only for assessing large forest areas and mapping or opening new forest land, but

92 particularly for measuring individual trees and stands in order to derive quantitative  
93 measurements required for forest management, such as tree height and crown diameter.  
94 Investigating the potential applications of airborne laser scanner data is another important  
95 focus of current research. Other methods have also been used to measure 3D data, including  
96 optical stereo and radar systems.

97

98 Most of the work carried out to date has focused on forestry (Lim and Honjo, 2003; Disney  
99 et al., 2006; Simard et al., 2008; Ling and Jie, 2008; Kushida et al., 2009). However, 3D  
100 models may also be valuable in agricultural landscapes, with some applications being  
101 similar to those used in forest areas and others being specific to agricultural subjects. The  
102 special characteristics of agricultural crops make it difficult to apply some techniques to  
103 forest plantations. One basic difference relates to the accessibility of the zones of study for  
104 people and vehicles. Forest areas are often difficult to access for people and especially for  
105 vehicles. However, the transit of both people and machinery within agricultural plantations  
106 is guaranteed in most cases. This is highly relevant as, it largely determines the kinds of  
107 instrumentation that can be used in each case. This explains the use of 3D LIDAR sensors  
108 in ground-based laser studies for forest applications.. The main advantage of using these  
109 sensors is that they provide a three-dimensional cloud of points of the measured object.  
110 However, the high cost of these instruments limits their use.

111

112 In agricultural applications, however, it is possible to use two-dimensional (2D) terrestrial  
113 LIDAR sensors, which are much cheaper to use (Walklate et al.,2002; Palacín et.al., 2007).  
114 2D LIDAR sensors obtain a cloud of points corresponding to a plane or section of the  
115 object of interest. Sensor position, when well-determined (for example, with a constant

116 known-speed linear movement) allows the registration of measurement results  
117 corresponding to different planes or cross sections of the object, generating a 3D point  
118 cloud.

119

120 The objective of this work is to explain how to use 2D terrestrial LIDAR to obtain the 3D  
121 structure of agricultural plants, trees and canopies in a digital format.

122

## 123 **2. Materials and methods**

124

### 125 *2.1. System description*

126 The scanner used was a general-purpose Sick LMS200 model: a 2D divergent laser scanner  
127 with a maximum scanning angle of 180°, with a selectable lateral resolution of between  
128 0.25°, 0.5° and 1° and an accuracy of  $\pm 15$  mm in a single-shot measurement and a 5 mm  
129 standard deviation in a range of up to 8 m. The distance between the laser scanner and the  
130 object of interest was determined by measuring the time interval between an outgoing laser  
131 pulse and the return signal reflected by the target object. Fig. 1 shows a scheme with the  
132 main components of the experimental LIDAR system, while Table 1 summarizes the  
133 outstanding characteristics of LMS 200 LIDAR.

134

### 135 *2.2. Development of measurement software*

136 Specific software was developed to control the LMS200 laser scanner and to collect, store  
137 and process the data measured by the sensor. In the initial development stage, the LIDAR  
138 was interfaced to a computer through a RS232 serial port for data recording and offline

139 processing using a graphic interface developed in MatLab (The Mathworks Inc, Natick,  
140 MA). In the final test stage, the LIDAR was interfaced to a Compact FieldPoint  
141 programmable automation controller (National Instruments Corporation, Austin, TX) for  
142 real time operation.

143

144 The LIDAR was used to obtain vertical slices of the tree surface. Each vertical slice was  
145 composed of the points of intersection between the laser beam and the vegetation. The  
146 distance between slices when the system runs at  $1 \text{ km.h}^{-1}$  is of 20 mm. With a lateral  
147 resolution of  $1^\circ$ , the vertical distance between consecutive measurements lies within a range  
148 of 10 to 50 mm, depending on the distance between the LIDAR and the measured object.

149 Raw data generated by the LMS-200 LIDAR can be configured in two different modes: i)  
150 only by distance or ii) by distance and reflectivity. For the proposed application, the  
151 LIDAR was configured in the distance only mode, and the sensor data were composed of  
152 the radial distance corresponding to each angular direction of laser beams (polar  
153 coordinates).

154

155 The integration of sensor data measured at different LIDAR positions into one coordinate  
156 system for obtaining the 3D structure of plants was carried out as explained below. Firstly,  
157 the spatial coordinates of the point of intersection of each laser beam with the plant were  
158 measured with respect to the LIDAR. For each LIDAR position, the intersection points  
159 corresponding to a full  $180^\circ$  LIDAR scan gave the slice contour of the plant for that  
160 position. The exact position of each slice contour along the tree row (y-axis, Fig 2) was  
161 determined by the time between slices and from the forward travel speed of the LIDAR  
162 (which was attached to a mobile structure or tractor), which was kept constant in each trial.

163 In the case of field tests, the speed of the tractor was kept constant by means of its manual  
164 velocity control, and its real value was determined by GPS measurements. As a result, the  
165 accumulation of the slice contour set of points along the tree row produced a cloud of plant  
166 intersection points. Although the LMS200 LIDAR is a 2D laser scanner, the software that  
167 has been developed has made it possible to use it as a 3D scanner by moving the sensor in a  
168 direction parallel to the row of trees at a known speed. After subsequently converting the  
169 polar coordinates of the intersecting points supplied by the LIDAR to Cartesian  
170 coordinates, the program exported the x,y,z Cartesian values of each data point in a file  
171 format ready to be used by the most common CAD, GIS, statistical and computational  
172 software, thereby making 3D modelling and data processing very simple. One of the  
173 options of the program allowed us to georeference the data obtained by introducing the  
174 real-time coordinates of the LIDAR sensor measured using a GPS system. However, this  
175 option is only useful if the GPS system to be used offers precision to within only a few cm.

176

### 177 *2.3. Laboratory tests.*

178 The developed system was tested in a laboratory. The laser scanner was fixed to a mobile  
179 structure suspended from the ceiling and its linear velocity could be selected by the user. In  
180 this way, the LIDAR was able to follow a straight path at a known speed when scanning the  
181 object being studied. The first laboratory tests produced 3D measurements of the geometric  
182 dimensions (width, height and thickness) of solid objects, such as a PVC tube and a steel  
183 frame. The results obtained with the LMS200 LIDAR system were then compared with  
184 manual measurements of the same objects. Laboratory measurements of a medium size tree  
185 (a *Ficus Benjamina Variegata* approximately 2 m. high, 0.7 m. wide and with a foliage  
186 density similar to that of common Mediterranean fruit trees) were subsequently carried out



187 in order to test the performance of the measurement system in a controlled and reproducible  
188 environment. The *Ficus* was placed inside a steel frame with vertical and horizontal wires  
189 that made it possible to divide the plant into 36 cubes for subsequent defoliation. The laser  
190 moved in a straight line, with minimum distance of at least 1 metre between the trunk of  
191 the plant and the path of the LIDAR sensor. Laboratory tests were carried out at two  
192 LIDAR angular resolutions ( $1^\circ$  and  $0.5^\circ$ ) and three advance speeds ( $0.5$ ,  $1$ , and  $1.5 \text{ km.h}^{-1}$ ).  
193 Both the front and rear of the *Ficus* were scanned using the laser system.

194

#### 195 *2.4. Measurements with real crops*

196 Field measurements with real tree crops were made in 2004 and 2005. Before that, a device  
197 was designed that made it possible to accommodate the LMS200 laser scanner on a vertical  
198 axis at different heights above the soil surface. This device had four wheels so that it could  
199 be moved manually. Alternatively, the system could be mounted in the back of a tractor.  
200 Fig. 2 shows the experimental system used for field measurements.

201 Each field test consisted of several runs (measurements) along either side of the row, with  
202 the LIDAR mounted in the back of a tractor and moving in a straight line at a constant  
203 known speed (between  $1 \text{ km.h}^{-1}$  and  $2 \text{ km.h}^{-1}$ ) and a distance of between 1 m and 3 m from  
204 the trees axis, depending on the crop measured, as shown in Fig. 3. The interval of the  
205 scanning angle of the LIDAR was between  $0^\circ$  and  $180^\circ$ , and two different ( $0.5^\circ$  and  $1^\circ$ )  
206 angular resolutions were used. For each crop, the laser sensor was placed at three different  
207 heights, depending on the geometric characteristics of the plants in question (0.9 m, 2.1 m  
208 and 3.3 m, in the case of fruit trees and 1.2 m, 1.6 m and 2.0 m, in the case of vineyards).  
209 The ground surface of the travel path was quite smooth due to frequent tractor travel and  
210 compaction. The measured area contained several trees and had a total length of between

211 1.2 and 40 m, depending on the crop. Some known objects were placed, for reference  
212 (reference planes), at the exact points where measurements began and ended. These were  
213 wooden structures with flat surfaces that the LIDAR detected correctly and they served as  
214 references for analysis and the subsequent processing of data. By joining together each  
215 cloud of points obtained from the scanner measurements made on both sides of the trees,  
216 and following the procedure described in the next paragraphs, it was possible to obtain 3D  
217 images of the crops.

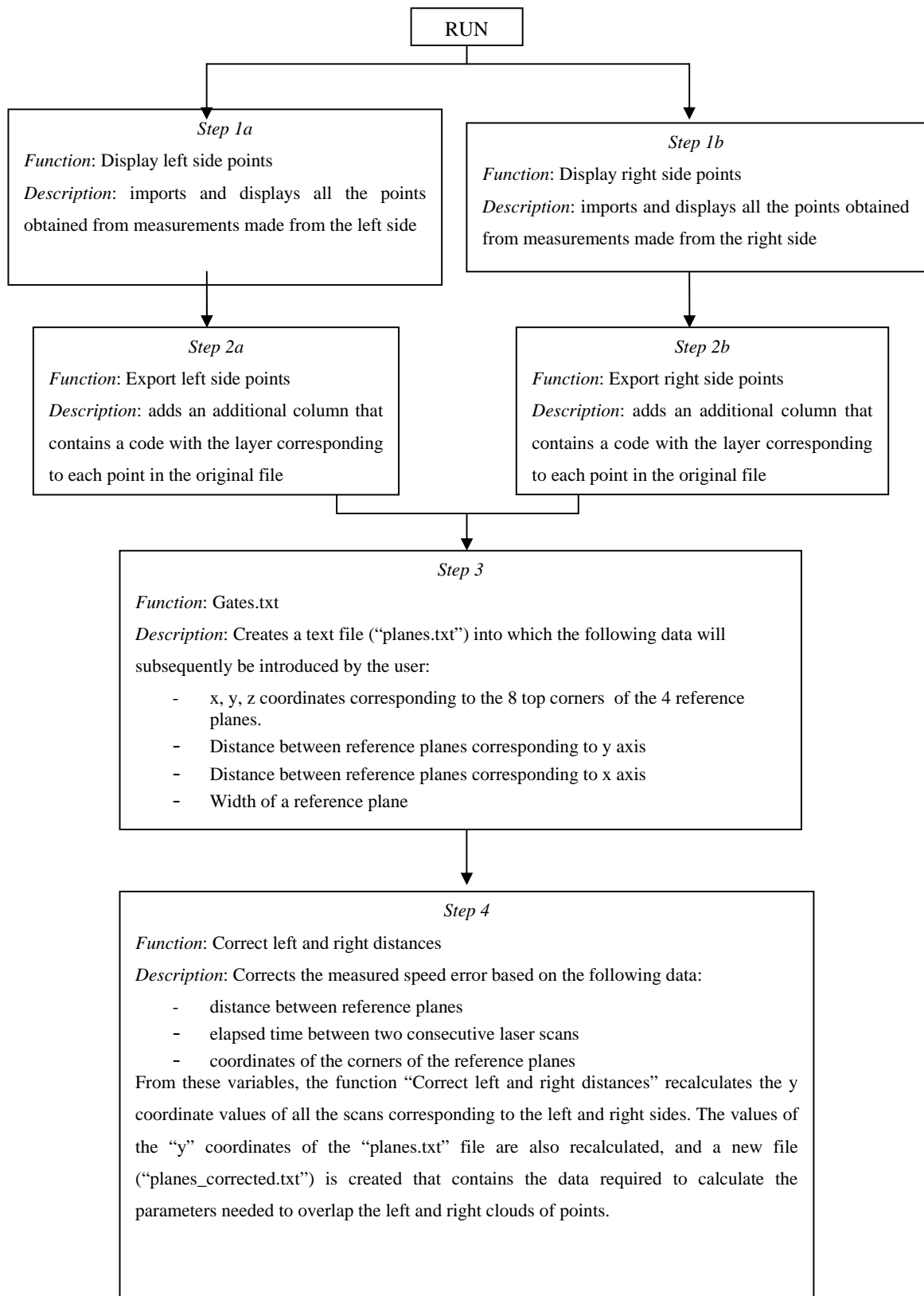
218

#### 219 *2.5. Construction of 3D models of plants*

220 Each cloud of points obtained from LIDAR measurements corresponding to a side (left or  
221 right) of the trees was independent. Each cloud of points therefore had its own coordinate  
222 origin, which coincided with the position of the sensor when measurement started. In order  
223 to build 3D models of plants, it was necessary to overlap the points of the two sides of the  
224 plants. This implied that all the points obtained had to be registered in a single coordinate  
225 system and that the points obtained from one of the measured sides had to be transferred to  
226 the coordinate system of the other. The superposition and display of the two clouds of  
227 points corresponding to the two sides of the plants was carried out using an automated  
228 procedure followed by a manual adjustment.

229

230 In the automated phase, the clouds of points were processed using specific software that  
231 automatically overlapped them. This software was developed by the authors in VBA  
232 (Visual Basic for Applications), making use of the programming resources of AUTOCAD  
233 (Autodesk, Inc.). The following flow chart explains how this software works:



235 In order to illustrate this procedure, the upper part of Fig 4 shows two clouds of points  
236 corresponding to the left and right side measurements of a crop, with each in its own  
237 coordinate system. The lower part of Fig 4 shows the superposition of the two clouds of  
238 points corresponding to both sides of the plants in the same coordinate system.

239

240 Some additional errors could be produced in field tests as a consequence of inaccuracies in  
241 the following experimental steps: positioning the vertical bar that holds the LIDAR sensor;  
242 levelling the LIDAR; setting the reference planes; keeping the speed and trajectory of the  
243 sensor constant and keeping its path straight. Other external factors, including: vibration  
244 of the sensor due to soil irregularities; changes in slope and soil roughness; the movement  
245 of leaves and branches caused by the tractor and/or the wind also influenced measurements.

246

247 In some cases, such human and environmental influences factors had a detrimental effect  
248 on the overlap of the two side measurements and therefore subsequent fine adjustments  
249 were needed to improve it. Such errors were corrected after the automated superimposition  
250 had been completed by making fine manual adjustments to the superimposed figures. This  
251 manual adjustment involved four movements of the cloud of points on the left-hand side:

252

- 253 - y axis rotation
- 254 - (Vertical ) displacement on the z axis
- 255 - (Horizontal) displacement on the x axis
- 256 - (Horizontal) displacement on the y axis

257

258 The quantification of these movements was based on the locations of common elements  
259 that were present in measurements made on both sides of the plants: the soil, the lower part  
260 of the trunk, the leafless areas of plants, poles, wires, and individual branches, etc.

261

262 Figs. 5a) and 5b) illustrate the fine adjustment process. The clouds of points corresponding  
263 to the left and right sides are respectively represented in red and green. The example has  
264 been deliberately exaggerated in order to facilitate understanding of the fine adjustment  
265 process. The magnitude of this kind of error is usually much smaller.

266 The manual process starts when an unsatisfactory overlap (upper left corner of Fig. 5a)  
267 needs a more precise adjustment. Taking the common soil zones shown in the images  
268 obtained from the two as a reference, we carried out an anti-clockwise rotation of  $3^\circ$  around  
269 the y axis on the left side of the figure (upper right corner of Fig. 5a). We then carried out a  
270 displacement of 73 mm on the left side of the figure, along the z axis (lower left corner of  
271 Fig. 5a). Subsequently, based on the reference planes, a displacement of 50 mm of the left  
272 side figure along the x axis is done (lower right corner of Fig. 5a). In this example, due to  
273 the low foliage density of the plants, the LIDAR sensor (despite being located on the left  
274 side) measured points corresponding to laser impacts on the reference planes located on the  
275 right side, and vice versa. This also makes it possible to correct the x axis. Finally, the  
276 upper part of Fig. 5b) shows a front view of the same crop, just before the adjustment along  
277 the y axis. Based on the perimeter contours of the leafless areas of plants, displacing the left  
278 side figure 125 mm along the y axis produced the definitive cloud of points, with a front  
279 view which is represented in the lower part of Fig. 5b).

280

281 The previously mentioned corrections affect the following systematic errors (which are  
282 constant during the tests): a) position in height and levelling of the LIDAR sensor, b) lack  
283 of precision in the reference planes position, and c) different tractor speeds when scanning  
284 the left and right sides. The correction of non-systematic errors, such as soil irregularities,  
285 the zigzagging of the tractor, the variations in speed during measurement etc., requires the  
286 use of more sensors in the system, such as clinometers, gyroscopes or high precision GPS.  
287 It is also necessary to create new software to automatically identify and correct these errors.  
288

289 After obtaining the preliminary results of tests carried out in 2004, the LIDAR system was  
290 applied in the 2005 season to characterize some common Spanish tree crops. The species  
291 analyzed were: pear trees (*Pyrus communis* L. 'Conference' and 'Blanquilla'), apple trees  
292 (*Malus communis* L. 'Red Chief' and 'Golden'), vineyards (*Vitis vinifera* L. 'Cabernet  
293 Sauvignon' and 'Merlot') and citrus (*Citrus reticulata* Blanco 'Oronules' 'Fortune' and  
294 'Marisol'; and *Citrus sinensis* L. cv. Osb Navelate).  
295

### 296 **3. Results and discussion**

297 There was a good degree of agreement between the results corresponding to solid objects  
298 obtained with LIDAR and by manual measurements. This can be seen from comparisons  
299 between the real dimensions of the steel frame (Fig. 6) used in the laboratory tests and  
300 those extracted from LIDAR measurements. The width and height of the steel frame were  
301 measured by both the manual and LIDAR procedures at several points in the structure.  
302 Differences between the real dimensions of the steel frame and those obtained using

303 LIDAR were within  $\pm 15$  mm. This was compatible with the system error stated in the  
304 technical specifications of the LMS 200 laser scanner (Table 1).

305

306 The same system error was found for LIDAR measurements of individual vegetation  
307 components (leaves and branches) under both laboratory and field conditions. However, a  
308 detailed study of laser beam characteristics and its interaction with leaves showed that  
309 when the laser beam partially impacted on two leaves, under certain conditions, instead of  
310 giving the distance to the first object, it provided an intermediate distance between the two.

311 A laser beam is able to simultaneously impact on two (or even more) plant components  
312 because it is several centimetres wide. In fact, due to laser beam divergence, its cross  
313 section (and therefore the probability of partial simultaneous impact) tends to increase with  
314 distance (for example, transversal beam width increased from 2 cm to 3 cm when the  
315 distance from the LIDAR increased from 2 m. to 4 m.). Whether or not the sensor gave the  
316 distance to the first object or to an intermediate value depended on the distances between  
317 the LIDAR, first, and second object, and also on the distribution of laser intensity. Thus,  
318 despite the previously explained restrictions, from the results obtained from laboratory  
319 tests, it is possible to conclude that the LIDAR system was able to measure the geometric  
320 characteristics of plants with sufficient precision for most agriculture applications. Fig. 8  
321 shows an example of a 3D image obtained from a laboratory test.

322

323 As a result of the developed work, a system capable of obtaining the three-dimensional  
324 structure of trees and plantations was obtained and used to characterize real crops. The  
325 results of field measurements, undertaken in 2004 and 2005 seasons, which were conducted

326 for several types of tree crops (pear trees, apple trees, citrus and vineyard crops) made it  
327 possible to obtain 3D digitalized images of crops, from which a large amount of plant  
328 information -such as height, width, volume, leaf area index and leaf area density- could be  
329 obtained. Figs. 7 and 8 show some examples of the images obtained, which were taken with  
330 a digital camera and the developed LIDAR system. These figures show great concordance  
331 between the physical dimensions, shape and global appearance of the 3D digital plant  
332 structure and real plants and reveal the coherence of the 3D tree model obtained from the  
333 developed system with respect to the real structure. This high level of agreement is shown  
334 more explicitly in Fig. 9, where the concordance of the physical dimensions and shape of  
335 both foliated branches and leafless areas is very high. The top of Fig. 9 shows the volume  
336 occupied by the cloud of points. For some selected trees, the correlation coefficient  
337 obtained between manually measured volumes and those obtained from the 3D LIDAR  
338 models was as high as 0.976 (e.g. in the case of pear trees, *Pyrus communis* L.  
339 'Blanquilla'). Furthermore, repetitions of these measurements produced similar results. For  
340 example, a second test for pear trees produced a correlation coefficient for manual versus  
341 laser-estimated volumes of 0.974: very similar to the previous value.

342

343 As explained, the methodology developed made it possible to obtain a satisfactory three-  
344 dimensional structure of trees and crops in an appropriate format for multiple uses. There  
345 is, however, still room to improve the procedure for obtaining 3D images. Indeed, as  
346 previously expounded, these images are obtained from known, fixed reference points (the  
347 reference planes) and by subsequently overlapping the measurement results corresponding  
348 to each side. This procedure is, however, very time-consuming, as several steps must be  
349 carried out manually. Much effort is currently being made to achieve measurements and



350 results that can be obtained automatically and without the need to use the planes of  
351 reference. This will be possible as soon as GPS systems provide the required level of  
352 accuracy at a moderate cost. If, in addition, it is possible to incorporate precision  
353 inclinometers into the system, it will also be possible to convert it into a portable 2D  
354 ground LIDAR system for the 3D characterization of plantations.

355

356 Likewise, as far as the software is concerned, tools for automatically differentiating  
357 between herbs, trunks, branches, leaves and the ground are being developed. At present,  
358 this task has to be carried out manually. The same occurs with determinations of the plant  
359 volume and other parameters of interest: the newly developed tool will allow these  
360 determinations with precision, but still manually and in a time consuming way. Future  
361 efforts must therefore also focus on developing tools that can carry out these determinations  
362 faster and more automatically.

363

#### 364 **4. Conclusions**

365 This paper examines the use of a 2D LIDAR scanner in agriculture to obtain three-  
366 dimensional characteristics of trees and crops. The results obtained for fruit orchards, citrus  
367 orchards and vineyards show that this technique could provide fast, reliable, and non-  
368 destructive estimates of 3D crop structure. As a result, it was possible to obtain a three-  
369 dimensional cloud of points, drawn by CAD software. This format facilitated data handling  
370 for both qualitative and quantitative studies of the geometric parameters of plants. There  
371 was a great degree of concordance between the physical dimensions, shape and global  
372 appearance of the 3D digital plant structure and the real plant. The correlation coefficient  
373 between manually measured plant volume and that obtained using the 3D LIDAR model

374 was also high. The precision and repeatability of the measurements obtained led us to the  
375 conclusion that the newly developed LIDAR measurement system would be suitable for a  
376 wide range of applications in agriculture. This tool could constitute a valuable instrument  
377 for scientists, since it makes it possible to introduce the ground-based remote measurement  
378 of the three-dimensional structure of plants (geometry, size, height, cross-section, etc) as a  
379 complementary variable in their research. Once the 3D structure has been obtained,  
380 numerous applications are possible. The geometric (height, volume, etc) and structural  
381 (Leaf Area Index -LAI-, Leaf Area Density, etc) characteristics of plants, as well as their  
382 temporal evolution, can therefore be determined with this non-destructive remote sensing  
383 technique. Reliable and objective estimations of Leaf Area Density and Leaf Area Index  
384 (LAI) are essential for accurate estimations of canopy carbon gain by trees. A 3D  
385 representation of tree-covered fields can also help to improve our knowledge of their  
386 characteristics and offer a valuable aid for making decisions and extracting conclusions as  
387 well as helping to improve the representation of plant-related information in Geographical  
388 Information Systems.

389

390 Future research will be directed towards developing tools to differentiate between herbs,  
391 trunks, branches, leaves and the ground and towards quickly and automatically constructing  
392 GPS-supported 3D models of plants and 3D maps of tree crops. In this way, the physical  
393 characteristics of a crop that has been measured with the LIDAR system could be compared  
394 and integrated with other geo-referenced information relating to the same crop (satellite  
395 data, disease distribution maps, yield maps, etc).

396

397

398

399 **Acknowledgements**

400 *This research was funded by the CICYT (Comisión Interministerial de Ciencia y*  
401 *Tecnología, Spain), under Agreement No. AGL2002-04260-C04-02.*

402

403 *LMS200 and SICK are trademarks of SICK AG, Germany.*

404

405

406

407

408

409

410

411

412

413

414

415

416

417

418

419

420

421

422 **References**

423

424 Andersen, H., Reng, L., Kirk, K., 2005. Geometric plant properties by relaxed stereo vision  
425 using simulated annealing. *Computers and Electronics in Agriculture* 49, 219-232.

426

427 Aschoff, T., Thies, M., Spiecker, H., 2004. Describing forest stands using terrestrial laser-  
428 scanning. In: Conference proceedings ISPRS conference. ISPRS International Archives of  
429 Photogrammetry, Remote Sensing and Spatial Information Sciences Vol XXXV, Part B,  
430 Istanbul, Turkey, 12 – 23 July 2004, pp. 237-241.

431

432 Blair, J.B., Rabine, D.L., Hofton, M.A., 1999. The laser vegetation imaging sensor : a  
433 medium-altitude, digitisation-only, airborne laser altimeter for mapping vegetation and  
434 topography. *ISPRS Journal of Photogrammetry and Remote Sensing* 54, 115-122.

435

436 Bongers, F., 2001. Methods to assess tropical rain forest canopy structure: an overview.  
437 *Plant Ecology* 153, 263-277.

438

439 Bradbury, R., Hill, R., Mason, D., Hinsley, S., Wilson, J., Balzter, H., Anderson, G.,  
440 Whittingham, M., Davenport, I., Bellamy, P., 2005. Modelling relationships between birds  
441 and vegetation structure using airborne LiDAR data: a review with case studies from  
442 agricultural and woodland environments. *Ibis* 147, 443-452.

443

444 Coops, N.C., Hilker, T., Wulder, M.A., St-Onge, B., Newnham, G., Siggins, A., Trofymow,  
445 J.A., 2007. Estimating canopy structure of Douglas-fir forest stands from discrete-return  
446 LiDAR. *Trees, Structure and Functions* 21(3), 295-310. doi: 10.1007/s00468-006-0119-6.  
447

448 Disney, M., Lewis, P., Saich, P., 2006. 3D modelling of forest canopy structure for remote  
449 sensing simulations in the optical and microwave domain. *Remote Sensing of Environment*  
450 100(1), 114-132.  
451

452 Fleck, S., Van der Zande, D., Schmidt, M., Coppin, P., 2004. Reconstructions of tree  
453 structure from laser-scans and their use to predict physiological properties and processes in  
454 canopies. In: ISPRS WG VIII/2 Workshop “Laser-Scanners for Forest and Landscape  
455 Assessment”. ISPRS International Archives of Photogrammetry, Remote Sensing and  
456 Spatial Information Sciences, Vol XXXVI-8/W2, Freiburg, Germany, 3-6 October 2004,  
457 pp.119-123.  
458

459 Fröhlich, C., Mettenleiter, M., 2004. Terrestrial laser-scanning- New perspectives in 3D-  
460 surveying. In: ISPRS WG VIII/2 Workshop “Laser-Scanners for Forest and Landscape  
461 Assessment”. ISPRS International Archives of Photogrammetry, Remote Sensing and  
462 Spatial Information Sciences, Vol XXXVI-8/W2, Freiburg, Germany, 3-6 October 2004,  
463 pp. 7-13.  
464

465 Giles, D.K., Delwiche, M.J., Dodd, R.B., 1989. Sprayer control by sensing orchard crop  
466 characteristics: orchard architecture and spray liquid savings. *Journal of Agricultural  
467 Engineering Research* 43, 271–289.

468

469 Giuliani, R., Magnanini, E., Fragassa, C., Nerozzi, F., 2000. Ground monitoring the light  
470 shadow windows of a tree canopy to yield canopy light interception and morphological  
471 traits. *Plant Cell Environment* 23, 783-796.

472

473 Gobakken, T., Næsset, E., 2008. Assessing effects of laser point density, ground sampling  
474 intensity, and field sample plot size on biophysical stand properties derived from airborne  
475 laser scanner data. *Canadian Journal of Remote Sensing* 38, 1095-1109.

476

477 Houldcroft, C., Campbell, C., Davenport, I., 2005. Measurement of canopy geometry  
478 characteristics using LiDAR laser altimetry: a feasibility study. *IEEE Transactions on*  
479 *Geoscience and Remote Sensing* 43(10), 2270-2282.

480

481 Kise, M., Zhang, Q., 2006. Reconstruction of a virtual 3D field scene from ground-based  
482 multi-spectral stereo imaging. In: *Proceedings of the 2006 ASABE Annual International*  
483 *Meeting, Portland, Oregon. Paper Number 063098.*

484

485 Kushida, K., Yoshino, K., Nagano, T., Ishida, T., 2009- Automated 3D forest surface  
486 model extraction from balloon stereo photographs. *Photogrammetric Engineering and*  
487 *Remote Sensing* 75(1), 25-35.

488

489 Leblanc, S., Chen, J., Fernandes, R., Deering, D., Conley, A., 2005. Methodology  
490 comparison for canopy structure parameters extraction from digital hemispherical  
491 photography in boreal forests. *Agricultural and Forest Meteorology* 129, 187-207.

492

493 Lee, A., Lucas, R., Brack, C., 2004. Quantifying vertical forest stand structure using small  
494 footprint LIDAR to assess potential stand dynamics. In: ISPRS WG VIII/2 Workshop  
495 "Laser-Scanners for Forest and Landscape Assessment". ISPRS International Archives of  
496 Photogrammetry, Remote Sensing and Spatial Information Sciences, Vol XXXVI-8/W2,  
497 Freiburg, Germany, 3-6 October 2004, pp. 213-217.

498

499 Li, F., Cohen, S., Naor, A., Shaozong, K., Erez, A., 2002. Studies of canopy structure and  
500 water use of apple trees on three rootstocks. *Agricultural Water Management* 55, 1-14.

501

502 Lim, E.M., Honjo, T., 2003. Three-dimensional visualization forest of landscapes by  
503 VRML. *Landscape and Urban Planning* 63(3), 175-186.

504

505 Ling, Z., Jie, Z., 2008. Obtaining three-dimensional forest canopy structure using TLS.  
506 *Proceedings of SPIE-The International Society for Optical Engineering*. Vol. 7083, Article  
507 number 708307.

508

509 Næsset, E., 1997a. Estimating timber volume of forest stands using airborne laser scanner  
510 data. *Remote Sensing of Environment* 61, 246-253.

511

512 Næsset, E., 1997b. Determination of mean tree height of forest stands using airborne laser  
513 scanner data. *ISPRS Journal of Photogrammetry and Remote Sensing* 52, 49-56.

514

515 Næsset, E., 2009. Effects of different sensors, flying altitudes, and pulse repetition  
516 frequencies on forest canopy metrics and biophysical stand properties derived from small-  
517 footprint airborne laser data. *Remote Sensing of Environment* 113, 148-159.

518

519 Parker, G., Harding, D., Berger, M., 2004. A portable LIDAR system for rapid  
520 determination of forest canopy structure. *Journal of Applied Ecology* 41, 755-767.

521

522 Palacin, J., Palleja, T., Tresanchez, M., Sanz, R., Llorens, J., Ribes-Dasi, M., Masip, J.,  
523 Arnó, J., Escolà, A., Rosell, J.R., 2007. Real-time tree-foliage surface estimation using a  
524 ground laser scanner. *IEEE Transactions on Instrumentation and Measurement* 56(4), 1377-  
525 1383.

526

527 Pereira, A., Green, S., Villa Nova, N., 2006. Penman-Monteith reference evapotranspiration  
528 adapted to estimate irrigated tree transpiration. *Agricultural Water Management* 83, 153-  
529 161.

530

531 Pfeifer, N., Gorte, B., Winterhalder, D., 2004. Automatic reconstruction of single trees  
532 from terrestrial laser scanned data. In: Conference proceedings ISPRS conference, ISPRS  
533 International Archives of Photogrammetry and Remote Sensing, Vol. XXXV, B5, Istanbul,  
534 Turkey, 12 – 23 July 2004, pp. 114-119

535

536 Phattaralerphong, J., Sinoquet, H., 2004. A method for 3D reconstruction of tree canopy  
537 volume from photographs: assessment from 3D digitised plants. In: Proceedings of the 4th



538 International Workshop on Functional-Structural Plant Models, Montpellier, France, pp.  
539 36-39.  
540  
541 Rovira-Más, F., Zhang, Q., Reid, J., 2005. Creation of Three-dimensional Crop Maps based  
542 on aerial stereoisimages. *Biosystems Engineering* 90(3), 251-259.  
543  
544 SICK AG, 2002. LMS 200/LM S211/ LMS 220/ LMS 221/ LMS 291 Laser Measurements  
545 Systems. Technical Description.  
546  
547 Simard, M., Rivera-Monroy, V.H., Mancera-Pineda, J.E., Castañeda-Moya, E., Twilley,  
548 R.R., 2008. A systematic method for 3D mapping of mangrove forests base don Shuttle  
549 Radar Topography Mission elevation data, ICESat/GLAS waveforms and field data:  
550 Application to Ciénaga Grande de Santa Marta, Colombia. *Remote Sensing of Environment*  
551 112(5), 2131-2144.  
552  
553 Solanelles, F., Escolà, A., Planas, S., Rosell, J.R., Camp, F., Gràcia, F., 2006. An electronic  
554 control system for pesticide application proportional to the canopy width of tree crops.  
555 *Biosystems Engineering* 95(4), 473–481.  
556  
557 Solberg, S., Naesset, E., Lange, H., Bollandsas, O., 2004. Remote sensing of forest health.  
558 In: ISPRS WG VIII/2 Workshop “Laser-Scanners for Forest and Landscape Assessment”.  
559 International Archives of Photogrammetry, Remote Sensing and Spatial Information  
560 Sciences, Vol XXXVI-8/W2, Freiburg, Germany, 3-6 October 2004, pp. 161-166.  
561

562 Stuppy, W., Maisano, J., Colbert, M., Rudall, P., Rowe, T., 2003. Three-dimensional  
563 analysis of plant structure using high-resolution X-ray computed tomography. Trends in  
564 Plant Science 8(1), 2-6.

565

566 Tanaka, T., Park, H., Hattori, S., 2004. Measurement of forest canopy structure by a laser  
567 plane range-finding method. Improvement of radiative resolution and examples of its  
568 application. Agricultural and Forest Meteorology 125, 129-142.

569

570 Van der Zande, D., Hoet, W., Jonckheere, I., Van Aardt, J., Coppin, P., 2006. Influence of  
571 measurement set-up of ground-based LiDAR for derivation of tree structure. Agricultural  
572 and Forest Meteorology 141(1), 147-160.

573

574 Walklate, P.J., Cross, J.V., Richardson, G.M., Murray, R.A., Baker, D.E., 2002.  
575 Comparison of different spray volume deposition models using LIDAR measurements of  
576 apple orchards. Biosystems Engineering, 82(3), 253-267.

577

578 Yu, X., Hyypä, J., Kaartinen, H., Hyypä, H., Maltamo, M., Rönholm, P., 2005.  
579 Measuring the growth of individual trees using multitemporal airborne laser scanning point  
580 clouds. In: ISPRS WG III/3, III/4, V/3 Workshop "Laser scanning 2005", Enschede, the  
581 Netherlands, September 12-14, pp. 2005.

582

583 Zaman, Q.U., Salyani, M., 2004. Effects of foliage density and citrus speed on ultrasonic  
584 measurements of citrus tree volume. Applied Engineering in Agriculture 20(2), 173-178

585

586 Zaman, Q., Schumann, A., 2005. Performance of an ultrasonic tree volume measurement  
 587 system in commercial citrus groves. Precision Agriculture 6(5), 467-480.

588

589

590

591

592 **Table 1.** Characteristics of LMS200 laser scanner (SICK AG, 2002)

593

<b>Wave length</b>	905 nm
<b>Maximum range</b>	8 or 80 m
<b>Angular resolution</b>	0.25° / 0.5° / 1°
<b>Response time</b>	53 ms / 26 ms / 13 ms
<b>Measurement Resolution</b>	±10 mm
<b>System error</b>	Typ. ± 15 mm, range 1 ...8 m
<b>(environmental conditions: good visibility, T<sub>a</sub>=23°C, reflectivity ≥ 10%)</b>	Typ. ± 4 cm, range 1 ...20 m
<b>Statistical error, standard deviation (1 sigma)</b>	Typ. ± 5 mm (at range ≤ 8m / ≥10 % reflectivity / ≤ 5 kLux
<b>Temperature</b>	0°C ..... 50°C
<b>Data transmission rate</b>	9.6 / 19.2 / 38.4 / 500 kBauds
<b>Weight</b>	4.5 kg

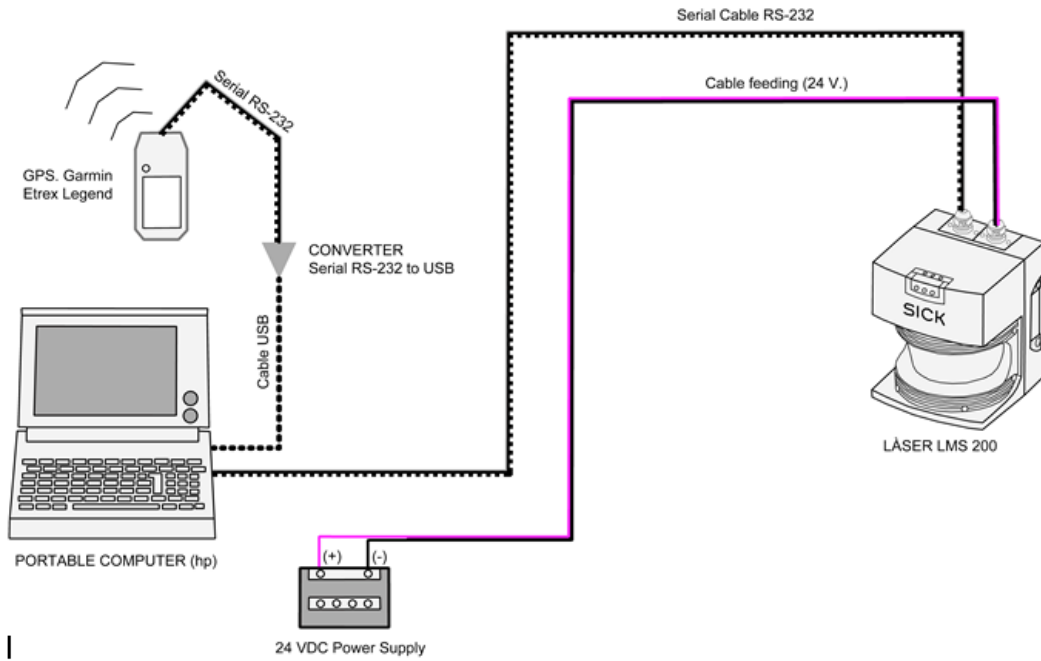
594

595

596

597

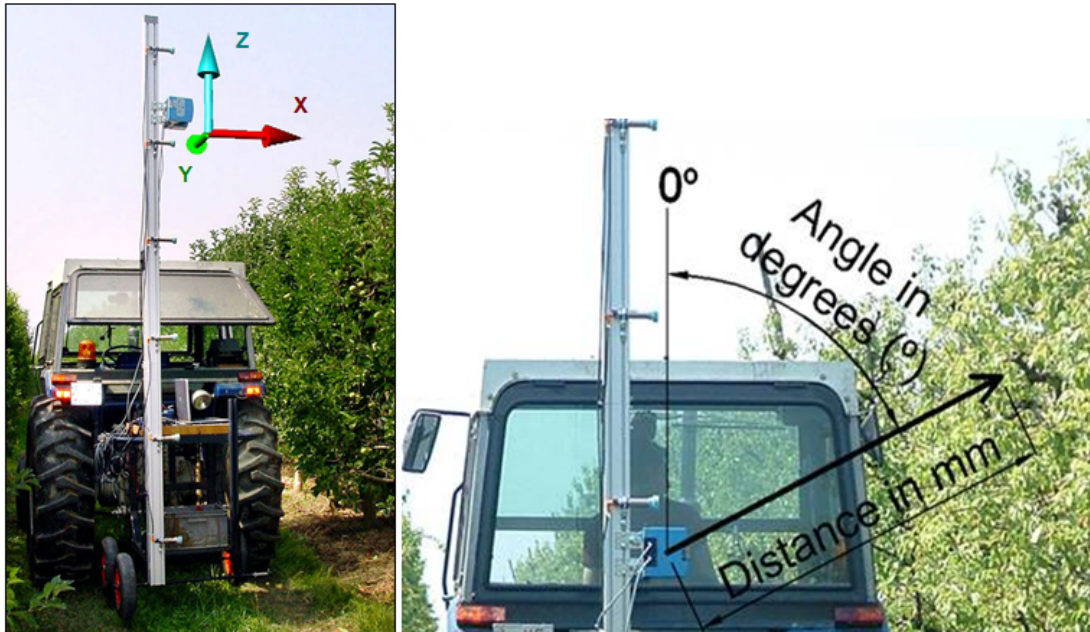
598



599  
600

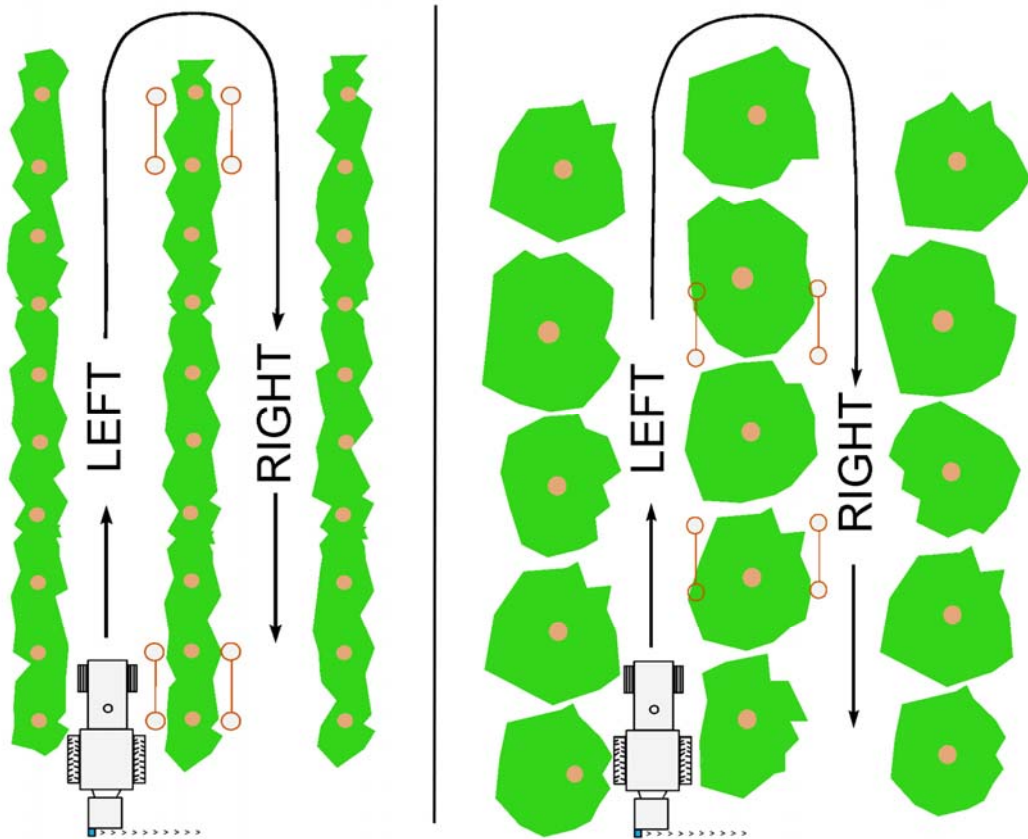
601 **Fig. 1.** A scheme of the main components of the experimental LIDAR system

602  
603



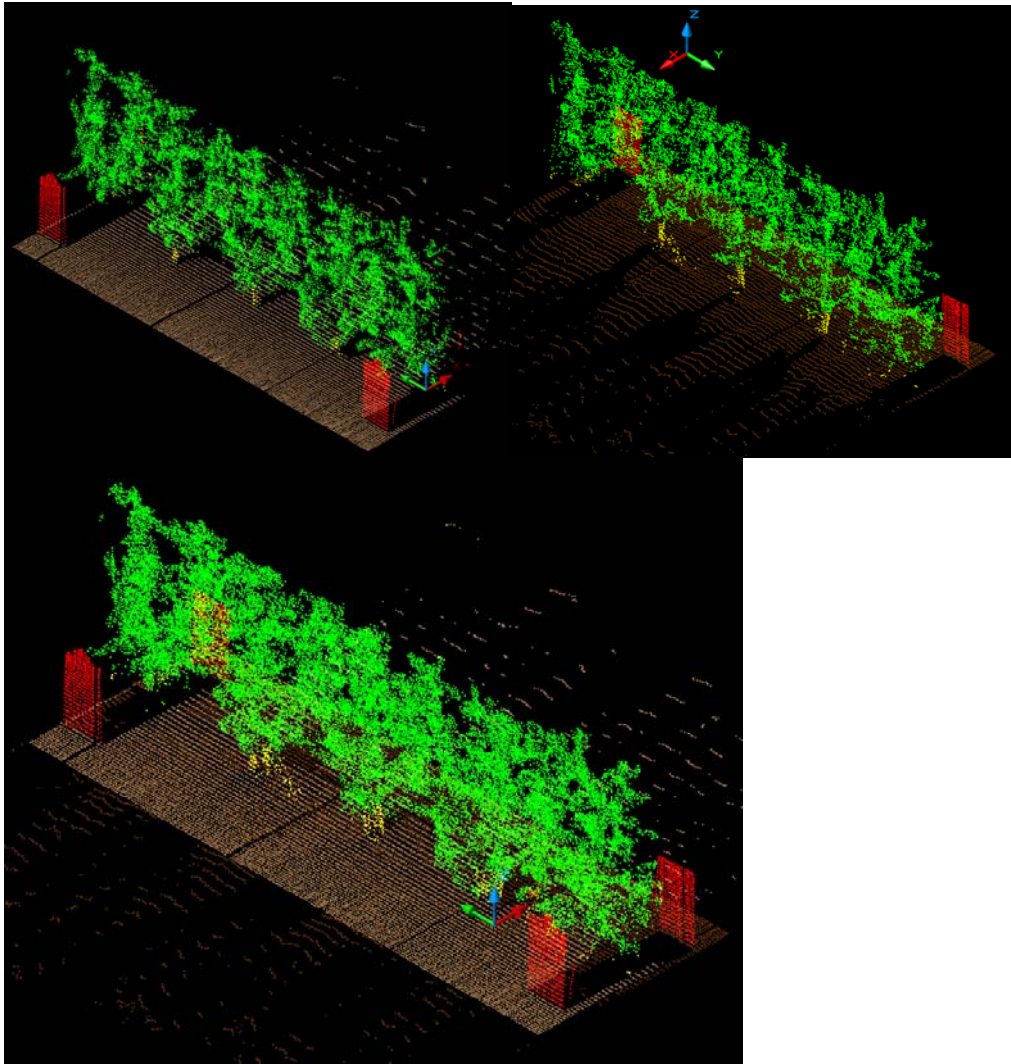
604  
605  
606  
607  
608  
609  
610  
611  
612  
613  
614  
615  
616  
617  
618  
619

**Fig. 2.** The LIDAR measurement system, mounted on a tractor, carrying out an experimental test in a pear orchard. Six ultrasound distance sensors are also shown. The height of the laser sensor above the ground was between 0.9 m and 3.3 m, depending on crop characteristics and the purpose of the test. The measurement data formats are also shown. *Left:* data in Cartesian coordinates: x, y, z (the y coordinate corresponds to the tractor displacement axis). *Right:* data in polar coordinates (distance and angle).



620  
 621  
 622  
 623  
 624  
 625  
 626  
 627  
 628  
 629  
 630  
 631  
 632  
 633

**Fig. 3.** Trajectory of the LIDAR measurement system on both sides of the tree rows. *Left:* fruit trees and vineyard orchards (almost continuous vegetation). *Right:* Citrus orchards and isolated trees (discontinuous vegetation).



634

635  
636  
637

638 **Fig. 4.** *Top left:* cloud of points corresponding to LIDAR measurements of a crop from the  
639 left side. *Top right:* cloud of points corresponding to LIDAR measurements of a crop from  
640 the right side. *Bottom:* superposition of the two clouds of points corresponding to the two  
641 sides in a single system of coordinates.

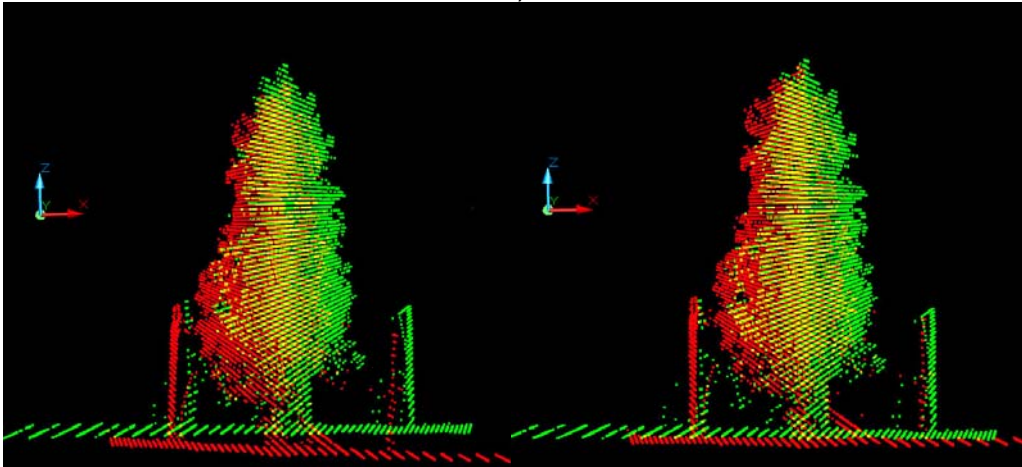
642

643

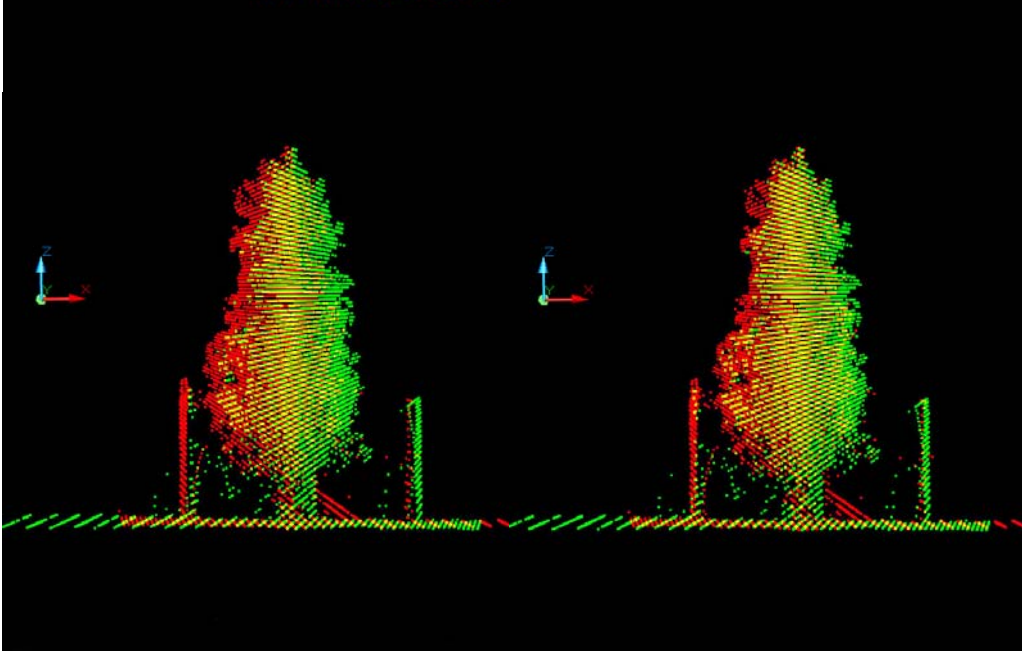
644

645

a)



646

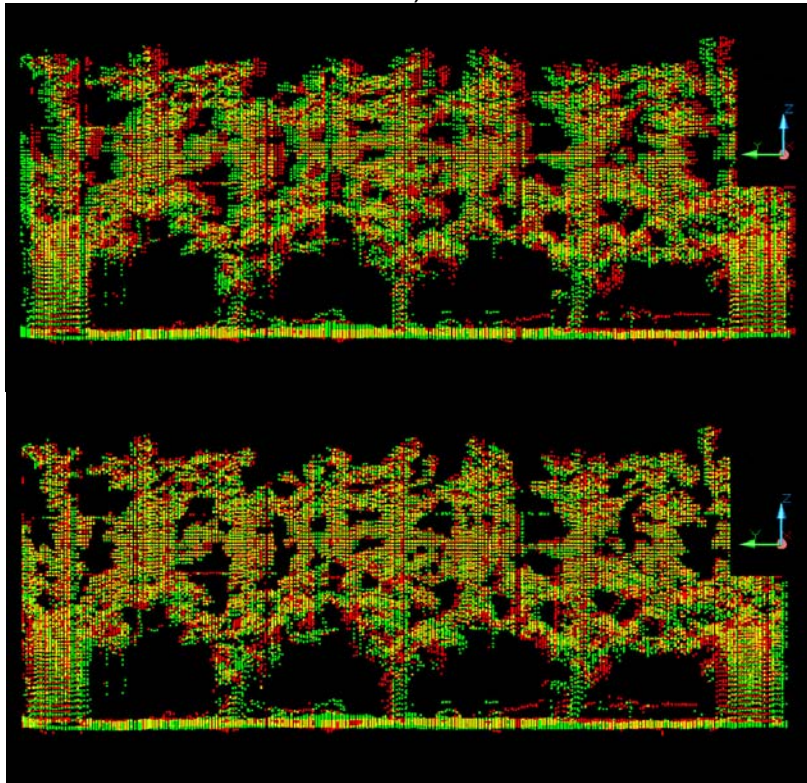


647  
648  
649  
650  
651  
652  
653  
654  
655  
656  
657  
658  
659  
660  
661



662  
663  
664  
665  
666

b)



667

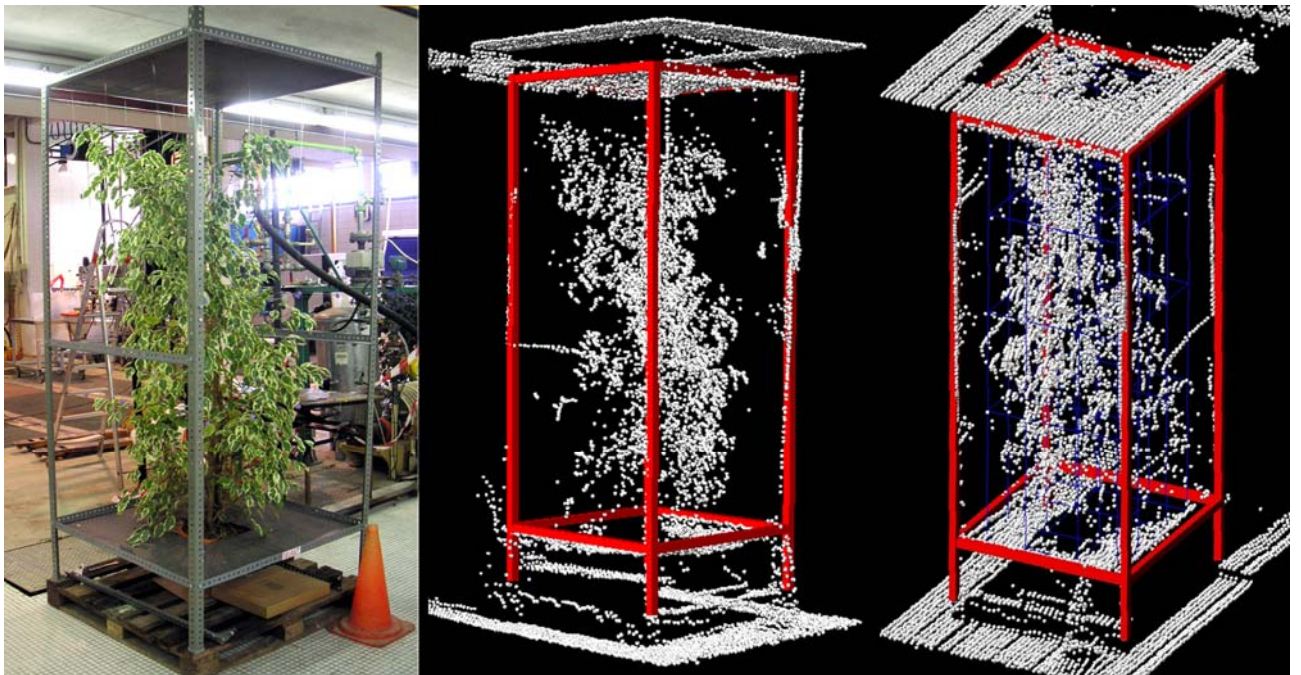
668  
669  
670

671 **Fig. 5. a)** Side view of a crop to illustrate the fine adjustment process. The clouds of points  
672 corresponding to the left and right sides are represented in red and green, respectively.  
673 Yellow points are the result of the visual confluence of red and green points. This figure  
674 shows the first three steps of the fine adjustment process for improving the overlap of the  
675 two clouds of points corresponding to the two sides of the plants. *Top left:* Initial situation  
676 of a fictitious example before any correction is implemented. *Top right:* The cloud of points  
677 after completing an anti-clockwise rotation of  $3^\circ$  around the y axis of the left side figure.  
678 *Bottom left:* The cloud of points after displacing the left side figure 73 mm along the z axis.

679 *Bottom right:* The cloud of points after displacing the left side figure 50 mm along the x  
680 axis.

681 *b)* Front view of a crop to illustrate the last step of the fine adjustment process. The clouds  
682 of points corresponding to the left and right sides are represented in red and green,  
683 respectively. *Top:* a front view of the clouds of points corresponding to both sides of the  
684 crop just before displacement along the y axis. *Bottom:* a front view of the definitive clouds  
685 of points after displacing the left side figure 125 mm along the y axis.

686



687

688

689

690 **Fig. 6.** Photography (*left*) and two 3D images (corresponding to different views) of a *Ficus*

691 *Benjamina Variegata*, obtained with a LMS200 laser scanner in a laboratory environment.

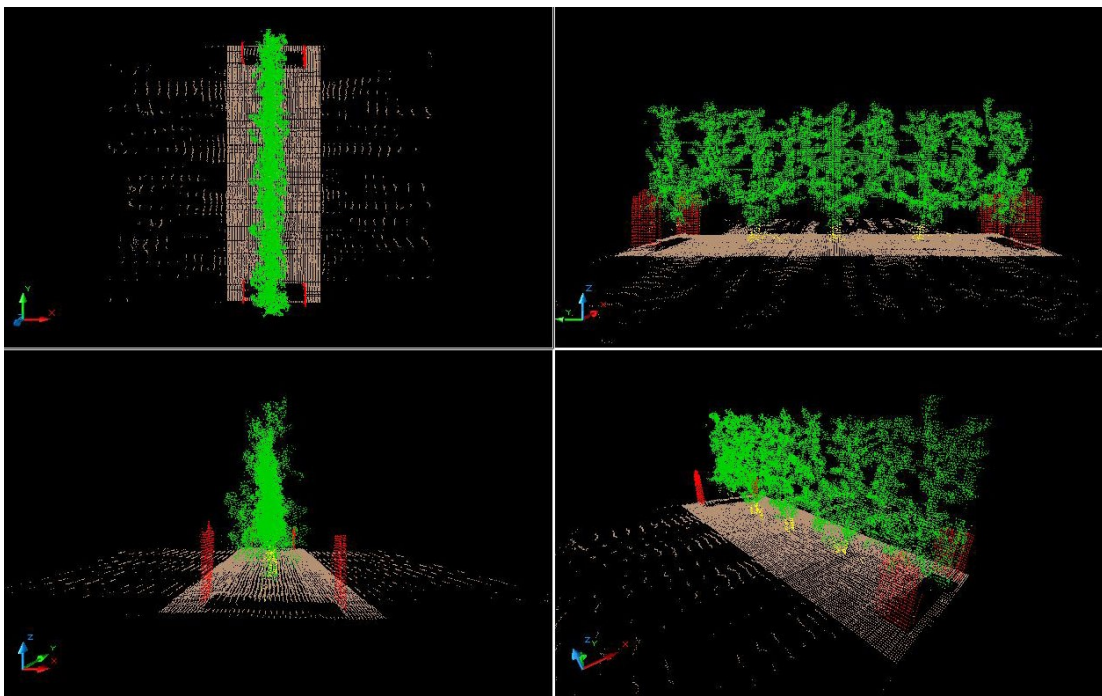
692

693

694

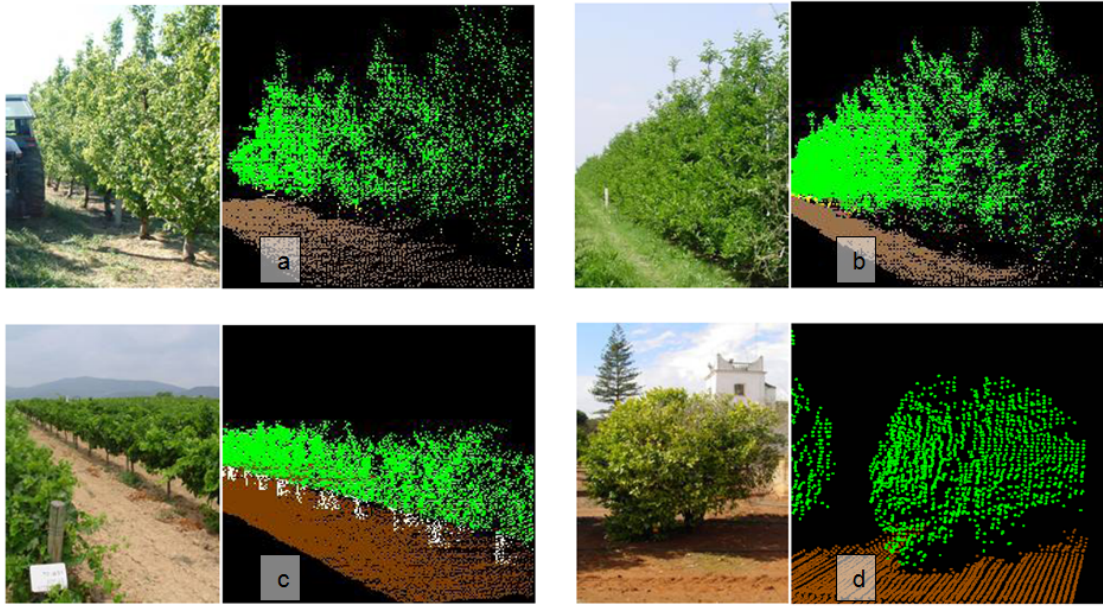


695  
696



697  
698  
699  
700

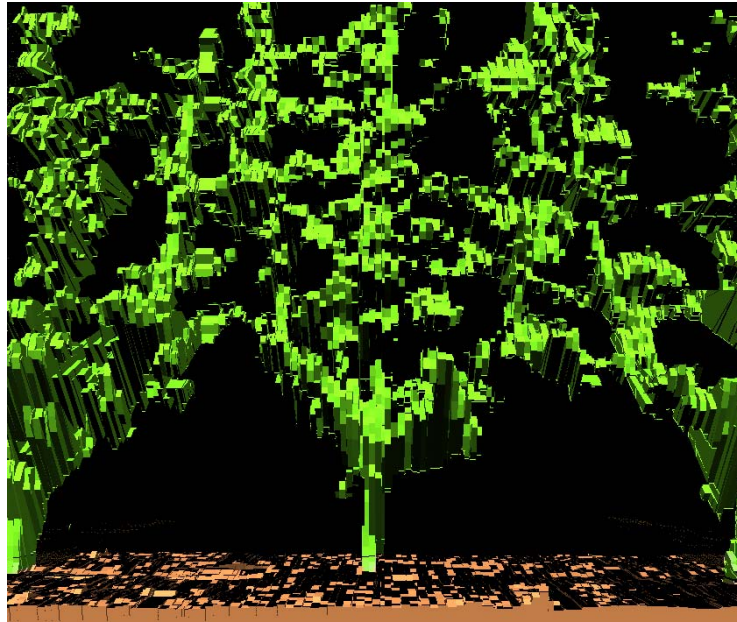
**Fig. 7.** Different views of the 3D structure of the pear orchard shown in the upper picture.



701  
702 **Fig. 8.** Pictures and 3D images of pear trees (a), apple trees (b), vineyards (c) and citrus  
703 trees (d).

704  
705  
706  
707  
708  
709  
710  
711  
712  
713

714



716  
717



718 **Fig. 9.** 3D model of pear trees (*Pyrus communis* L. ‘Blanquilla’) obtained from LIDAR  
719 measurements (*Top*) and digital photography of the same real trees (*Bottom*), evidencing  
720 the great degree of concordance between the two. The upper figure shows the volume  
721 occupied by the cloud of points.